Modelling microstructure formation in TiAl by isomorphic inoculation

J R Kennedy, Ahmed Kaci Boukellal, Miha Založnik, Dominique Daloz, Julien Zollinger

Modelling microstructure formation in TiAl by isomorphic inoculation

Modelling microstructure formation in TiAl by isomorphic inoculation

*** J.R. Kennedy[1,2], A.K. Boukellal[1], M. Založnik[1,2], D. Daloz[1,2], J. Zollinger[1,2]**

1 Université de Lorraine, Institut Jean Lamour, Department of Metallurgy and Materials Science and Engineering, Nancy, France

2 Laboratory of Excellence on Design of Alloy Metals for low-mAss Structures ('LabEx DAMAS'), France

Jacob.kennedy@univ-lorraine.fr

Abstract. Ti-Al alloys have replaced Ni-based superalloys in the last stages of some aircraft engines to improve fuel efficiency. In order to improve their properties, grain refinement has been investigated via isomorphic inoculation with Ti-Al-Nb particles. This inoculation method is orders of magnitude more efficient on a particle-by-particle basis than traditional inoculation, rather than multiple inoculant particles added to form a solidified bulk phase grain, in isomorphic inoculation each particle added results in the formation of multiple grains. As the particles are indistinguishable from the matrix after solidification, a model was used to elucidate this mechanism. Two phenomena were considered to calculate the number of particles acting during solidification: particle breakup along grain boundaries and complete particle dissolution. The grain size of the particles was calculated with an empirical model from initial TKD analysis of the particles and high temperature molten salt heat treatments. Particle dissolution was estimated via mass transport of the slowest diffusing Nb species. This showed the population of isomorphic inoculant particles which can act during solidification is near a 1:1 ratio with the number of grains formed, confirming the mechanism of grain refinement by direct epitaxial growth from the particles.

1. Introduction

The high specific strength and oxidation resistance of TiAl alloys make them particularly appealing for use in aerospace applications [1]. Currently they have been introduced in the last low pressure stage of the GEnx turbine engine as part of its goal to increase fuel efficiency. In order to better utilize these alloys grain refinement is needed, however, current methods rely on the introduction of brittle ceramic phases which act as inoculants [2]. Nucleation plays a key role when using such traditional inoculants for grain refinement. Inoculants facilitate heterogeneous nucleation as they reduce the activation energy required [3]. Models of heterogenous nucleation are broken into three main categories, spherical cap, free growth or constitutional supercooling [4]. In the first model, the effectiveness of the nucleant depends essentially on its characteristics. The kinetics are then determined by the formation of the nucleus and the adsorption rate of atoms into them. In the second model, heterogeneous nucleation is considered athermal and the active nucleants are determined by their size distribution. In the third, it is the constitutional undercooling at the front of growing crystals that triggers the active nucleants. In each case there is an energy barrier to the formation of new solid from the nucleant particles. In the case of slow solidification rates, predicting the grain size relies on linking both nucleation and crystal growth

in a complex manner, highly dependent on experimental conditions and alloy composition. Recent developments introduced isomorphic inoculants (ISI) as potential grain refiners for cast Ti-Al [5–7], these particles have a coherent interface with the solidifying bulk, as they solidify by epitaxial growth rather than nucleation of new solid, and are of the same phase, eliminating the need for brittle second phase particles. Such grain refiners also have potential to simplify prediction of as-cast grain size due to the suppression of the nucleation of new solid.

ISI particles are engineered alloy powders to grain refine during solidification without embrittlement. The ISI alloy is chosen such that at the temperature of a given melt they are of the same phase that will solidify while also being thermally stable [5]. The ISI alloy is then only effective when used for solidification of the phase it was designed for. The thermal stability of the ISI particles is achieved through refractory metal additions, in the case of the Ti-46Al (wt%) alloy investigated here the ISI alloy is Ti-10Al-25Nb (wt%). This alloy has a melting point above that of the bulk, 1800^{o}C compared to ~1540^{o}C, while existing as β-Ti, the TiAl alloy solidification phase, at high temperature. It is also important that the ISI particle density remains near that of the parent alloy or excess flotation or settling may occur preventing their active participation in solidification [6]. The mechanism of solidification from ISI particles differs from that of traditional inoculants which act as heterogeneous nucleation sites, but rather solidification occurs by epitaxial growth [8]. This results in solidification without a detectable interface between the particles and solidified bulk, and as such particles which participate in solidification cannot be detected ex-situ [7]. This is particularly interesting as since solidification is not occurring by nucleation of new solid, the energy barrier of nucleation is not encountered and as such particles of different sizes should induce solidification all at the same, minimal, undercooling as the only barrier to free growth is the strain from the difference in lattice parameters between the ISI alloy and bulk. This has interesting implications for validation of solidification models as each ISI particle added participates in solidification and should be responsible for the formation of an as-cast grain.

Casting trials of TiAl using TiAlNb ISI particles were carried out which showed each ISI particle added was responsible for the formation of multiple as-cast grains. Simple models were developed to account for the thermal and chemical effects of the ISI/melt interaction on the number of particles present during solidification. Taking into account these effects, the number of active ISI particles was used to predict the as-cast grain size assuming each particle formed a single grain.

2. Casting Trials

In order to test the efficacy of ISI particles as nucleant particles casting trials were carried out [5–7]. ISI particles were produced from commercially pure metals in an induction heated cold crucible apparatus as a bulk ingot. Drillings taken from the ingot were cryomilled for 3h under Ar and 3, 6, 9, or 11h under air to produce particles of different sizes. Particle size distributions had median (D50) sizes ranging from 233 μm (3h under Ar) to 48 μm (11h under air) as measured by SEM image analysis. There exists no simple way to add particles to the cold crucible apparatus used for the casting trials as melting and solidification are conducted under a high purity Ar atmosphere to prevent oxidation of the TiAl. In order to add the particles to the melt they were then mixed with pure Al powder in a 1:1 ratio and compressed to form a pellet which could held by means of a quartz vacuum tube until the TiAl was fully molten at which point the vacuum could be released and the pellet would fall into the melt. A target mass of 1g of ISI particles was added during each trial to TiAl ingots of roughly 40g. An interaction time of 20 s between the particles and melt was used in each trial to ensure there was no cooling effect from the particles on solidification. In each casting trial the grain size was reduced and equiaxed fraction increased compared to a reference ingot cast without ISI particles or accounting for the solutal effects of the Nb [5].

The as-cast grain size and equiaxed fraction, assuming spherical grains, can be used to calculate the number of equiaxed grains formed during solidification, while the size distribution of particles and mass of particles added yields the number ISI particles added. Figure 1 shows how these values compare across all casting trials. In conventional inoculation, where the inoculant particles act as heterogeneous nucleation sites, and as such an energy barrier exists in order for solid to grow from the

particles, the size distribution of inoculants is of critical importance, as the largest particles require the smallest undercooling to nucleate new solid they act first during solidification and the smallest particles are not active participants in solidification [9]. As such, the ratio of particles added to new grains formed is always less than 1:1, i.e., often 100 to 1000 or more particles need to be added to form a single new grain. This is in stark contrast to Figure 1 where in each trial more than 1 grain is formed by each particle added. It is then evident that further phenomena are occurring while the ISI particles are interacting with the melt to make this possible. While interacting with the melt the particles are subjected to both thermal and chemical conditions which will affect their properties. Both these factors must be accounted for in order to use ISI particles to predict the as-cast microstructure.

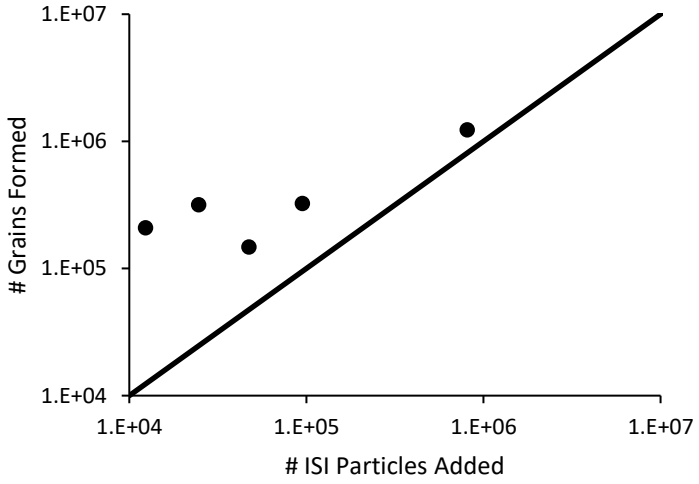

Figure 1: Relationship between the number of grains formed and number of ISI particles added

3. Thermal Effect: Particle Microstructure

Casting trials involving more highly stable TiTa particles which could survive prolonged contact with a TiAl melt revealed that dissolution was occurring preferentially along grain boundaries within the particles [6]. This is then likely also true of the TiAlNb particles used here which were processed in the same manner. The internal particle microstructures are then of critical importance. Initial investigations of the TiAlNb ISI particles by optical or SEM investigation did not have the resolution to reveal the internal microstructure of the particles. In order to evaluate the microstructure electron transparent samples was removed from 3h and 9h milled particles to be analysed by TEM and TKD. A TEM micrograph is shown in

Figure 2a from a 3h milled particle. The process of cryomilling resulted in a superplastically deformed nano-scale microstructure consisting of elongated grains after only 3h of milling. Further milling did not significantly change the grain size, however TKD analysis showed the fraction of low angle grain boundaries decreased with further milling, while high angle grain boundaries increased. The median grain size within the as milled particles was 35 nm [7].

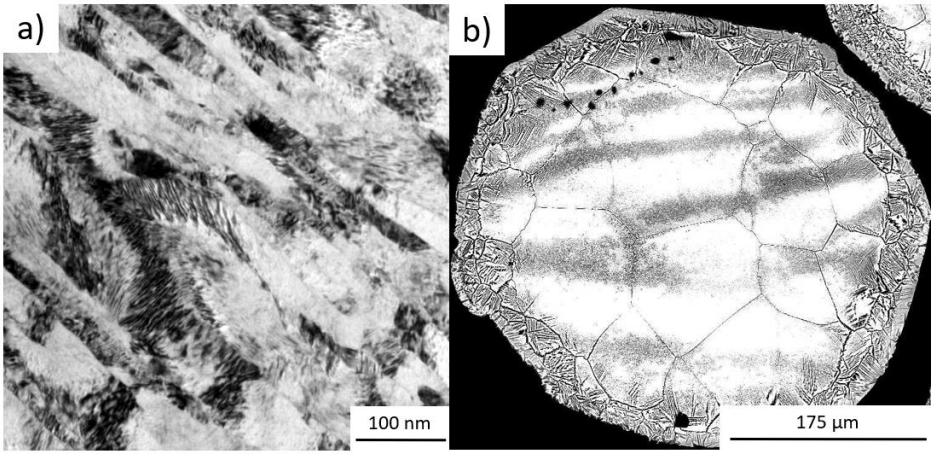

Figure 2: Microstructure of 3h cryomilled TiAlNb particles a) TEM micrograph of as milled particles and b) SEM BSE micrograph after 20s of interaction with molten CaF at 1600ºC

The thermal effects of the TiAl melt on the particle microstructures cannot be evaluated from the casting trials as the epitaxial growth mechanism made location of the original particles impossible. Furthermore, during the casting trials the particles were also subjected to the chemical effect of the melt. In order to evaluate the microstructure of the particles during solidification the thermal effect must be separated from the chemical effect. To that end a high temperature molten salt heat treatment was carried out on representative samples of 3h and 9h milled particles. A high temperature molten salt was chosen which did not react with the particles, CaF, and was stable at the melt temperature of 1600 ºC. In order to replicate the casting conditions alumina crucibles containing CaF were heated to 1600 ºC until the salt was completely melted then a representative sample of particles added to the CaF for 20s then quenched in water. After this heat treatment there was significant grain growth,

Figure 2b shows an SEM BSE micrograph of a 3h milled particle where the grain size has increased to be nearly 40 µm. These easily delineated interior grains were measured across multiple particles, both 3h and 9h milled, the results of which are shown in Figure 3. While the 9h milled particles tended to have smaller grain sizes, and the 3h larger, this corresponded to the 9h particles themselves also being smaller. The heat treated grain size was found to depend more on the size of the particles than their milling time, particles of similar size with either milling time had similar grain sizes. The average grain size across all the particles was found to be 37 µm, three orders of magnitude greater than the average as milled microstructure. A linear trend was observed between the particle size and interior grain size after heat treatment independent of milling time:

$$Gs=0.1069(Ps)+1.773$$

Where Gs is the resultant interior grain size and Ps the size of the milled particles. This trend could then be used to predict the grain size of particles after interaction with the melt.

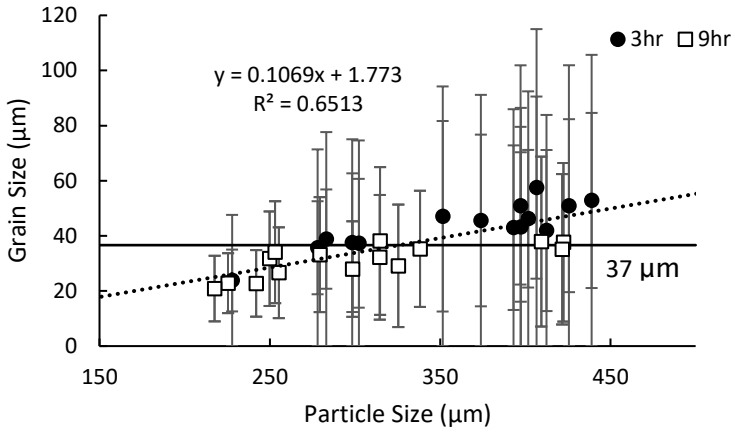

Figure 3: Measured grain sizes within particles of different sizes after replicating interaction with the melt.

4. Chemical Effect: Solid Dissolution

The design criteria of an ISI particle requires that they be thermally stable in the melt, i.e., their melting temperature is above that of the melt, however while the particles do not melt there is also the chemical effect of the molten TiAl which must be considered. Since preferential dissolution was observed in TiTa particles [6], it stands to reason that the particles also undergo partial or complete dissolution. As with the thermal effect, this cannot be evaluated from the casting trials alone. In order to evaluate the chemical dissolution of the particles a simple dissolution model was developed based on the work of Hsu and Lin [10], and validated through a rod dipping experiment.

4.1. Dissolution Model

A simplified first calculation model was developed to evaluate how dissolution is affecting the ISI particles. The casting trials were conducted in a complex environment, involving 3D fluid flow induced by the induction field, and the entire population of particles, these first calculations simplify the flow to 1D and the particle distributions are simplified to ten particle sizes each which do not interact with one another. In these calculations dissolution was according to film theory, i.e., the rate limiting step is the transport of the solute away from the interface [11]. This theory considers there is no solute buildup effect in the liquid, that it is an infinite medium. The model developed by Hsu and Lin builds upon film theory by also incorporating the volume of liquid the particles are interacting with, if solute buildup is a factor in the dissolution kinetics it is then considered [10]. Their model operates under the assumption that the dissolution rate is controlled by the transport of solute atoms through a boundary layer between the particles and the bulk liquid. This model was adapted for use with the ISI particles as shown in the schematic, Figure 4.

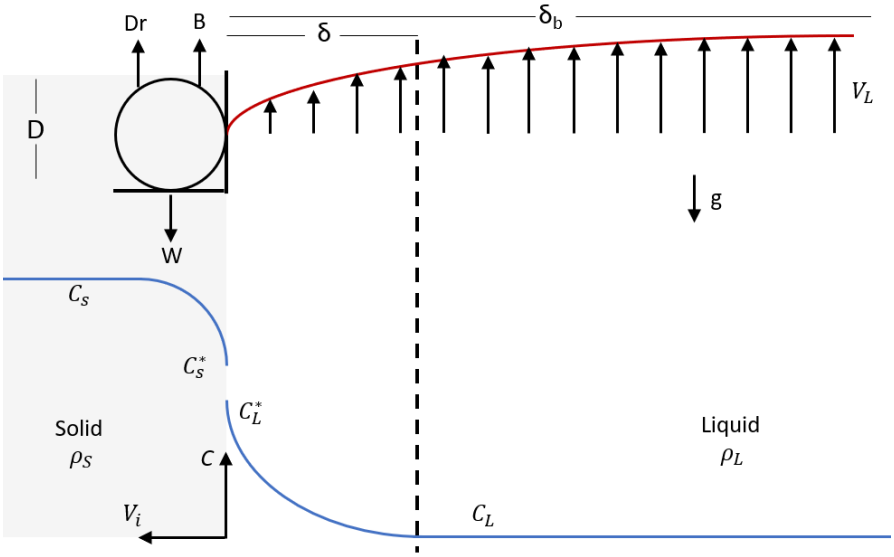

Figure 4: Schematic of dissolution model

The particles are not stationary in the melt, as such in order to calculate the width of the boundary layer their velocity relative to the liquid must be known. To simplify the 3D fluid flow only the maximum relative velocity, when the particle settling velocity is opposite that of the the liquid velocity, was considered. This was calculated by a force balance on the particle, shown in Figure 4, where the drag force (Dr) and buoyancy (B) act opposing the weight (W) of the particle. The relative velocity (V_{rel}) is then:

$$V_{rel} = \sqrt{4gD(\rho_s - \rho_L)/3C_D\rho_L}$$

where g is acceleration due to gravity, D is the particle diameter, ρ_s and ρ_L the particle and liquid density respectively and C_D the drag coefficient, which is dependent on the Reynolds number. As the particles remain in a laminar flow regime C_D can be taken as [12]:

$$C_D = 24/Re \quad Re < 53$$
$$C_D = 0.45 \quad 53 < Re$$

The initial velocity of the particles was taken to be the liquid velocity (assuming stationary particles) then the velocity, Reynolds number and drag coefficient calculations were iterated ten times, until variation was less than 1%. These values are needed to calculate the width of the fluid velocity boundary layer δ_b which is the distance from the particle where the fluid velocity returns to 99% of its free-flowing velocity. In reality this boundary layer around a sphere is non-uniform, compressed at the front of the particle and elongated in the rear. To simplify the boundary layer calculations the particles are instead considered to be cuboid and the boundary layer only considered on the faces parallel to V_{rel}, this is shown schematically in Figure 4. The mass transfer boundary layer taken to be the layer used for the dissolution calculations can be found by dividing the boundary layer by the Schmidt number yielding:

$$\delta = (D_L 5r)/(v\sqrt{Re})$$

Where δ is the mass transfer boundary layer, D_L the liquid diffusion rate of Nb, r the particle radius, ν the kinematic viscosity of the melt and Re the Reynolds number. The Nb diffusion rate in the liquid was calculated using the stokes-einstein relation as there is no literature data available. The thermophysical properties of our case required to implement the method of Hsu and Lin are given in Table 1.

Table 1: Thermophysical Properties for Dissolution Calculations

Variable	Symbol	Units	Value	Ref
Solute Liquid Diffusion	D_L	m^2/s	2.14×10^{-9}	PW
Particle Density	ρ_s	g/ m^3	5.01×10^6	[7]
Liquid Density	ρ_L	g/ m^3	3.82×10^6	[13]
Solute Molecular Weight	M	g/mol	93	[14]
Solute Liquid Concentration	C_L	mol/ m^3	0	PW
Solute Interface Concentration	C_i	mol/ m^3	8164	[15]
Kinematic Viscosity	ν	m^2/s	4.93×10^{-7}	[16]
Dynamic Viscosity	η	Pa s	1.88×10^{-3}	[16]
Temperature	T	^oC	1600	PW

4.2. Experimental Validation

A further experiment was needed to validate the dissolution of TiAlNb in molten TiAl using the above model. As with the thermal effect the addition of particles to the melt could not validate the model as the particles could not be located after solidification. A larger sample of TiAlNb which could be inserted into the melt, be easily located after solidification and would survive prolonged contact with the melt was needed. In order to fabricate such a sample a further bulk TiAlNb ingot was produced from pure elements in the same manner as for the ISI particles, a rod could then be produced by vacuum pulling. A quartz tube was inserted into the molten TiAlNb and a vacuum applied, the molten TiAlNb was pulled up the tube and solidified as a rod 5 mm in diameter and ~10 cm long. This rod could then be inserted into molten TiAl in a controllable manner under the same conditions as the casting trials, i.e., temperature and interaction time. The resultant rod/ingot assembly could be cross sectioned in order to measure the change in the rod diameter after interaction with the melt. An optical micrograph of the rod and measured radii along its length are shown in Figure 5. The average measured dissolution length after 20s of interaction with the melt at 1600^{o}C was 94 µm.

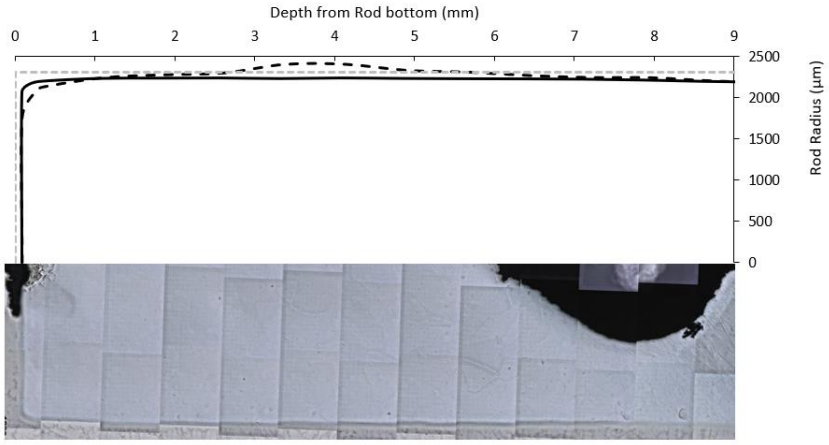

Figure 5: Optical micrograph and measured radii of TiAlNb rod after 20s interaction with melt. The grey line represents the initial radii and the black radii of either side of the rod after dissolution.

The details of the rod dipping were used in the dissolution model, namely the starting diameter of 5 mm, a length of 1 cm dipped into the melt and an interaction time of 20 s. The model then calculates the dissolution length over time as shown in Figure 6. After 20s of interaction with the melt the dissolution

length was 97 μm, close to the experimental value of 94 μm. This means the model and assumptions are reasonable for the given experimental conditions and can be applied to the real particle size distributions used in the casting trials.

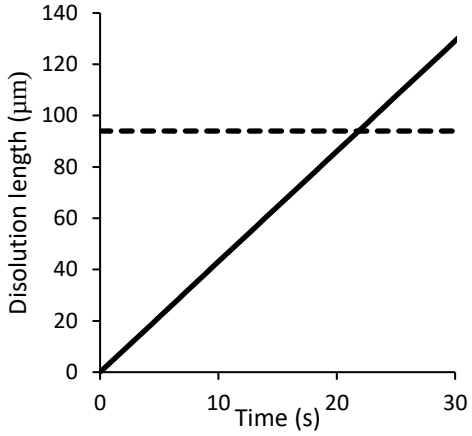

Figure 6: Calculated dissolution over time for TiAlNb rod in TiAl at 1600°C

5. Chemical and Thermal Effects on ISI Particles

The adapted model of Hsu for the chemical, dissolution, effect and the analytical grain size relation for the thermal, grain growth, effect can both then be applied to the ISI particle size distributions used in the casting trials. The known number of ISI particles added to the melt is increased by the thermal effect of grain growth/grain boundary dissolution, and simultaneously decreased by the chemical dissolution of some particles. Each of these effects is shown separately in Figure 7. Accounting for only thermal effects greatly increases the supposed number of active ISI particles, moving the distributions away from the 1:1 ratio of ISI: grains formed and into the regime of traditional inoculation [9]. In contrast accounting for only the thermal effect of particle dissolution moves the distributions further from 1:1 in the other direction with each particle responsible for even more new grains than previously. However, when both effects are considered, by firstly applying the chemical effect of particle dissolution then the thermal effect of grain growth on the dissolved particle sizes the ratio approaches 1:1, with the exception of the 11h milled sample. The median size of these particles, ~50 μm, is significantly smaller than that of the other distributions, ~110-230 μm, additionally in the case of the 11h milled particles the dissolution model predicts over 96% of the particles dissolving completely, this is likely an overestimation and results in fewer ISI particles predicted during solidification.

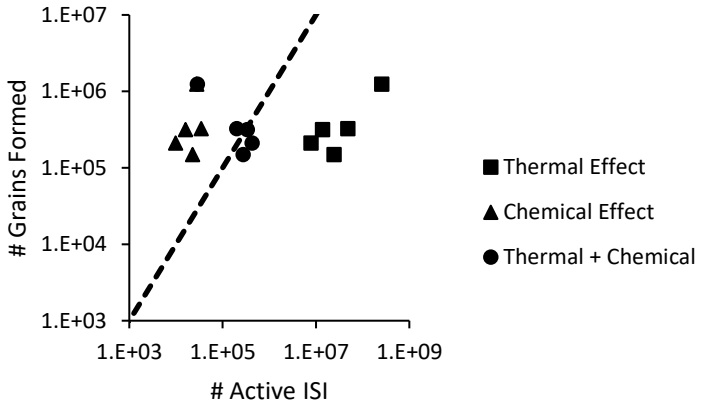

Figure 7: Relationship between the number of grains formed and number of ISI particles added considering different interaction phenomena

The calculated number of active ISI particles taking into account the chemical, thermal effects or both can then also be used to predict the as-cast grain size. Since ISI particles have been shown to induce solidification by epitaxial growth a 1:1 particle to grain relation can be inferred [8]. In the case of the casting trials the equiaxed volume of each ingot is known, so dividing this by the number of active ISI particles gives a grain volume which, assuming spherical grains, yields an estimated grain size. This is shown for each size distribution in Figure 8a considering: no interactions with the melt (particles introduced), only a thermal effect (grains introduced), only a chemical effect (particles remaining) or both a chemical and thermal effect (grains remaining). With the exception of the smallest introduced particle distribution considering both thermal and chemical effects predicts grain sizes most similar to those measured. However, the trend of predicted grain sizes increases with decreasing particle size while the experimental trials decrease grain size with decreasing particle size. This also points to an overprediction of the dissolution of small particles, leading to fewer predicted active ISI particles and larger predicted grain size. Even considering this it can be seen in Figure 8b that considering both thermal and chemical effects results in predictions closer to the experimental values. It is also interesting to note that when considering only the thermal, grain growth/ particle breakup, effect the predicted as-cast grain sizes are consistently 60-70% smaller than the experimental across all particle distributions. This indicates that there is a strong relationship between the internal grains of the particles and the as-cast grain size and that further work is needed to better estimate the dissolution of the particles to predict the grain size more accurately.

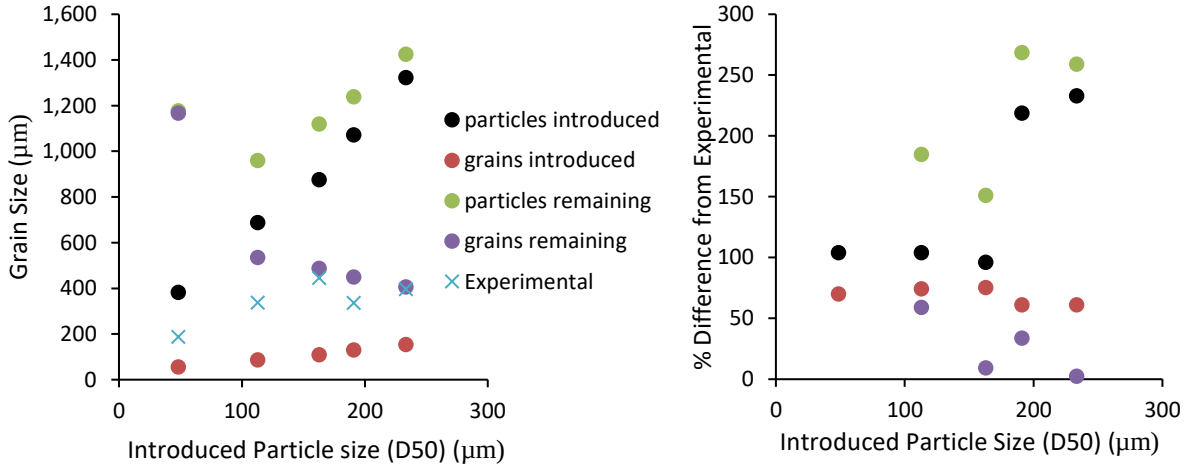

Figure 8: Predicted grain size and difference from experimental grain size for given introduced size distributions

6. Conclusions

ISI particles show significant potential as a tool to model as-cast grain size as they bypass the nucleation energy barrier by inducing solidification by epitaxial growth. However, the number of particles added to the melt does not correspond to the number of grains formed. This is due to both chemical and thermal effects of interaction between the melt and particles. The thermal effect of the interaction results in grain growth within the particles, which break up along their grain boundaries, while the chemical effect results in dissolution of some particles. Both these factors work together to change the number of active ISI particles present during solidification; dissolution decreases their number while particle breakup increases them. Taking into account both these effects using an empirical model for grain growth and a dissolution model based on the work of Hsu and Lin [10], the number of ISI particles present during solidification can be calculated. If the smallest particle size distribution is disregarded due to an overestimation of the dissolution of small particles, the predicted grain sizes are relatively close to those measured from experimental trials. In order to apply ISI particles to improve grain size modelling a dissolution model is needed which can account for dissolution of these small particles more accurately.

Additionally, the calculations could be simplified by manufacturing the particles using atomisation so each particle has a single grain rather than cryomilling which resulted in nano scale superplastically deformed grains.

References:

[1] Progress in the understanding of gamma titanium aluminides | SpringerLink, (n.d.). https://link.springer.com/article/10.1007/BF03221103 (accessed January 5, 2023).
[2] U. Hecht, V. Witusiewicz, A. Drevermann, J. Zollinger, Grain refinement by low boron additions in niobium-rich TiAl-based alloys, Intermetallics. 16 (2008) 969–978. https://doi.org/10.1016/j.intermet.2008.04.019.
[3] M. Rappaz, J.A. Dantzig, Solidification, EPFL Press, 2016.
[4] S.B. Park, Heterogeneous nucleation models to predict grain size in solidification, Prog. Mater. Sci. 123 (2022) 100822. https://doi.org/10.1016/j.pmatsci.2021.100822.
[5] J.R. Kennedy, D. Daloz, B. Rouat, E. Bouzy, J. Zollinger, Grain refinement of TiAl alloys by isomorphic self-inoculation, Intermetallics. 95 (2018) 89–93. https://doi.org/10.1016/j.intermet.2018.02.001.
[6] J.R. Kennedy, B. Rouat, D. Daloz, E. Bouzy, J. Zollinger, Effect of Inoculant Alloy Selection and Particle Size on Efficiency of Isomorphic Inoculation of Ti-Al, Materials. 11 (2018) 666. https://doi.org/10.3390/ma11050666.
[7] J.R. Kennedy, Development of a New Generation of Inoculants for Ti-Al Alloys, thesis, Université de Lorraine, 2018. http://www.theses.fr/2018LORR0101 (accessed April 20, 2020).
[8] J.R. Kennedy, A.E. Davis, A. Caballero, A. Garner, J. Donoghue, S. Williams, J. Zollinger, E. Bouzy, E.J. Pickering, P.B. Prangnell, Isomorphic grain inoculation in Ti-6Al-4V during additive manufacturing, Mater. Lett. X. 8 (2020) 100057. https://doi.org/10.1016/j.mlblux.2020.100057.
[9] T.E. Quested, A.L. Greer, The effect of the size distribution of inoculant particles on as-cast grain size in aluminium alloys, Acta Mater. 52 (2004) 3859–3868. https://doi.org/10.1016/j.actamat.2004.04.035.
[10] J.-P. Hsu, M.-J. Lin, Dissolution of solid particles in liquids, J. Colloid Interface Sci. 141 (1991) 60–66. https://doi.org/10.1016/0021-9797(91)90302-O.
[11] T.K. Sherwood, R.L. Pigford, C.R. Wilke, Mass transfer, McGraw-Hill, 1975.
[12] C.T. Crowe, Multiphase flows with droplets and particles, CRC Press, 2012.
[13] I. Egry, D. Holland-Moritz, R. Novakovic, E. Ricci, R. Wunderlich, N. Sobczak, Thermophysical Properties of Liquid AlTi-Based Alloys, Int. J. Thermophys. 31 (2010) 949–965. https://doi.org/10.1007/s10765-010-0704-1.
[14] P.T.B. Shaffer, Plenum Press Handbooks of High-Temperature Materials, Springer US, Boston, MA, 1963. https://doi.org/10.1007/978-1-4899-6405-2.
[15] V.T. Witusiewicz, A.A. Bondar, U. Hecht, T.Ya. Velikanova, The Al–B–Nb–Ti system, J. Alloys Compd. 472 (2009) 133–161. https://doi.org/10.1016/j.jallcom.2008.05.008.
[16] K. Zhou, H.P. Wang, J. Chang, B. Wei, Surface tension measurement of metastable liquid Ti–Al–Nb alloys, Appl. Phys. A. 105 (2011) 211. https://doi.org/10.1007/s00339-011-6491-0.